

## PROGRESS ON PREDICTIVE PERFORMANCE OF METAL CUTTING BY MACHINING PROCESSES - STUDY CASE: TURNING OPERATIONS THROUGH CONTROLLED CONTACT

Tonye K. Jack<sup>1</sup>, Aniedi O. Ette<sup>2</sup>, Aondona P. Ihom<sup>3</sup>

<sup>1,3</sup>Department of Mechanical and Aerospace Engineering, University of Uyo, Uyo, Akwa Ibom State, Nigeria  
<sup>2</sup>Department of Mechanical Engineering, Akwa Ibom State University, Ikot Akpaden, Akwa Ibom State, Nigeria

### Abstract

Studies on the development of models for the predictive performance of metal cutting by machining processes, initiated by CIRP, are currently ongoing at several research centers worldwide. This paper describes the successful outcomes achieved from primary research on the development of the ORTHO-OB CHATTER computer program, which enables data-driven predictive performance analysis of metal cutting by turning operations. Since data are critical to proper description of models, the work involved, gathering, generating and developing necessary support structured data that can be computationally applied through situated single- and multiple- input search queries, to predict generated forces, stresses, temperatures, strain rates, tool wear, possibility of fracture and tool life, stability and economic costs in lathe metal cutting involving any selected workpiece and tool materials combinations as a recommendation system to aid decision making. The paper also discusses predicting metal cutting operations under uncertainty by analyzing and identifying patterns and trends in data through mechanistic reasoning, providing a quick aid to help machinists select the correct size tools, cutting conditions, and make energy-saving decisions for a machining task. Validation shows errors in cutting force predictions by mechanistic reasoning of most material classes tested are within the range of zero to five percent.

**Keywords:** *Machining, Metal Cutting, Cutting Force Prediction, SMART Machining.*

### 1. Introduction

Accurate predictions of machining operations are surrounded by difficulties. With a set year of 2050 deadline, The Collège International pour la Recherche en Productique (CIRP) or The International Academy of Production Engineering initiated research and constituted a global experts committee in the last decade of the twentieth century, for completion of studies of models' developments for predictive performance of the metal cutting by machining processes to cover all the metal cutting process operations of turning, milling, drilling, grinding, and the more advanced machining processes, including high speed machining, with study guidelines to cover development of analytical, computer-aided (including Finite Element method), empirical, and integrated (combined) models for performance prediction of cutting forces, tool wear and fracture, tool-life, friction in the tool face, temperature distribution, surface roughness, chip type, and accuracy of machining finish of the work-piece [1]. The first working paper of the committee (van Luttervelt, Childs, Jawahir, Klocke, & Venuvinod, and others) [2] highlighted the likely difficulties of the study's exercise, with the vast number of variables in the metal cutting process, and the several non-formalized publications of knowledge bases of data

scattered all over the world. The ORTHOB-OB CHATTER computer program for predictive analysis of two-pass machining was developed through the application of data science for computer performance prediction in lathe turning operations.

### 2. Key considerations

The effects of the cutting conditions and tool geometry through the mechanics and thermal analysis of the chip formation process, the wear, and the likely final failure by fracture of the tool; stability effects due to vibration during the machining process, and the economic costs of the operation, all within an integrated analysis process. Principal concerns were machining under both dry and lubricated operating states, as well as the influence of the workpiece and tool materials' properties. In addition to selecting from list of existing shear angle theories for computational application, mimic models were derived to aid machining under cutting fluid conditions, based on reports by Shaw [1] that extensive research by several researchers shows that the chip thickness ratio,  $r_c$ , has the greatest influence on the friction coefficient,  $\mu$  – hence, the nonlinear cutting fluids models of:  $r_c = a\mu^b$  and  $r_c = aeb\mu$ , were applied by Jack [3] on data obtained from the open literature for several cutting fluid types. Workpiece and

\*Corresponding Author -E-mail: [tonyekjack@yahoo.com](mailto:tonyekjack@yahoo.com)

tool materials properties databases were developed for integrated dynamic data link analysis of the cutting process.

### 3. Databases

The workpiece materials database of the ORTHO-OB CHATTER computer program comprises a properties list of over 500 low, medium, and high carbon steels, alloy steels, stainless steels, special high-temperature nickel and titanium alloy steels, brass alloys, and plastics. The properties of interest are the mechanical, physical, thermal, and chemical properties, with a data size of (500 x 62) and (500 x 30), respectively. The tool materials' lists include over 90 tool types made up of High Speed Steel (HSS), Carbide, and Ceramic tools with a data size of (90 x 72). Additionally, properties data to aid fatigue and fracture analysis were included. Also of interest and listed are the typical common uses of the workpiece material. The default grading for workpiece materials for program analysis are the American Iron and Steel Institute (AISI) grades, but equivalent grades of other Countries where available, are listed for: Britain (British Standard - BS), Germany (Deutsches Institut für Normung – DIN, and Werkstoff-nummer - W-nr Standards), France (Association Française de Normalization - AFNOR), Italy (Ente Italiano di Unificazione - UNI Standard), Sweden (Svenska Intitutet för Standarder - SIS Standard), Japan (Japan International Standard - JIS), and China (Guo Bio – GB Standard). Warehoused structured, standardized, and non-standardized workpiece and tool materials properties data are extracted through drop-down buttons and loaded onto the solutions worksheet and transformed by application in the computation of desired cutting parameters for a metal cutting operation. Levels of semi-structured data types are provided and organized with flexibility to facilitate adaptable comparisons, offering exceptional value for gaining insights into theoretical differences and similarities in computational outcomes. An example is the various methods for computing the inclination angle in three-dimensional or oblique cutting. Additional examples are friction angle models for dry and lubricated cutting operations, monetary currency equivalents, and temperature rise factor models, among others.

### 4. Computer Program, Flowcharts, And Program Use

From the myriad of methods in the vast metal cutting literature for estimating certain key starting variables, such as specific cutting energy, shear angle, and shear plane yield shear stress, Microsoft Excel™

Worksheets suites of computer program modules were developed for analytical evaluation of orthogonal and oblique machining, taking into consideration variations in the different methods at estimation. The ORTHO-OB CHATTER program consists of ten orthogonal and nine oblique metal cutting by turning operations worksheets.

In Jack [3], guides on how to use the program and calculation format flow charts for each module are presented. Additionally, in Jack [3], validated and verified evidence across several classes of workpiece and tool material combinations under varied cutting conditions shows that accurate predictive outputs are method- and data-specific. Implying, for a defined set of cutting conditions, whilst machining some workpiece materials, with certain tool combinations, may predict cutting forces, temperature distributions, surface roughness, and tool life in close accordance with the experimentally accepted in a particular module of the ORTHO-OB CHATTER program, in other modules, the uncertainties may be very far removed. It will not be uncommon to attribute the errors in some modules to workpiece materials' non-linearity, since some laws of shear angle theories, while predicting well with experimental results when cutting a particular class of workpiece, have also been found to agree poorly when cutting other classes; this was also observed by Boothroyd [4]. However, evidence shows that, in the program modules initially predicting poorly, simulated variations of the defined set of cutting conditions result in better predictions of the desired cutting parameters. So, there is no consistency in the results output when predicting with different shear angle theories for the same cutting conditions.

The architecture for the calculation format as defined by the flow-chart for one such module in Jack [3] is presented in Fig. (1). Only the notations in the equations displayed in the flow-chart of Fig. (1) for the estimation of the cutting parameters to aid analysis of metal removal rates, cutting forces, and thermal effects are given in this paper. However, from the flowchart shown, it is evident that the ORTHO-OB CHATTER computer program is a comprehensive analytical program that can be used for surface finish calculation, machining vibration analysis, thermal analysis, machining economics evaluation, and tool wear and fracture analysis. In all, since there were many parameters to consider, a computationally intelligent or “SMART” (see Chartered Management Institute) [5] approach of “cause and effect” was adopted by Jack [3] in the mathematical model(s) applications and analysis. The guide for the “SMART” approach was that the requirements of a specific metal cutting operation be measurable with achievable and realistic cutting conditions for a good, final, acceptable machined product

surface roughness and finish within close tolerance, at a cost-effective machining time.

#### 4.1. Chip Breakage and Probable Tool Fracture

A fracture mechanics approach is adopted to predict chip separation/breakage and tool failure, bearing in mind that tool flank and crater wear precede the likely final tool failure. On the assumption that workpiece and tool materials inherently, are manufactured with pre-existing flaws, the Paris fatigue equation was applied to define the prediction of cycle lives or threshold of fracture by the threshold stress intensity factor difference:  $K_{ic} = (2.5E - 10/C)^{1/m}$ , and the eventual determination of the initial void or flaw sizes on the chip (assuming chip thickness single or double edged configuration cracks), and the tool (assuming inner centre-crack) prior to crack propagation. The factor, 2.5E-10 m/cycle, represents the crack growth rate per cycle suggested by Cookson [6], which defines the threshold level below which a crack will not propagate.

#### 4.2. Machining Economics

In terms of estimating machining cost analysis, the tools database includes averaged tool cost data for High-Speed Steel (HSS), Carbide, and Ceramic tools, strictly for estimation purposes, developed through a survey of online sources from several cutting tool sellers. The default monetary currency for tool cost price is the United States dollar, but the ORTHO-OB CHATTER computer program allows for exchange rate conversion to other monetary currencies. The monetary currencies selected for inclusion can be viewed as Continental representations. These are the British Pound, the Euro, the Swedish Kroner, the Swiss Franc, the Australian Dollar, the Canadian Dollar, the Japanese Yen, the Chinese Yuan, the Indian Rupee, the Saudi Riyal, the South African Rand, and the Nigerian Naira. An extension for the inclusion of other Countries' currencies is feasible. Estimation of the optimum tool life for maximum production efficiency or maximized profit rate is available in the computational iterative version of the program.

#### 4.3. Controlled-Contact Stability

One condition applied and taken as critical for cutting process stability is the controlled-contact condition ( $LSL \leq L_t$ ), based on the model of chip-tool friction in orthogonal cutting presented by Boothroyd [4], as shown by Fig. 2. The length of contact,  $L_t$ , at the tool-chip interface applied is of the form:

$$L_t = a_c \cdot \sin(\phi_n + \beta_n - \alpha_n) / \sin \phi_n \cdot \cos \beta_n \quad (1)$$

And the sliding length, LSL, model applied is as derived by Jack [3] in equation (2):

$$L_{SL} = L_t - L_{st} = L_t - L_t \left\{ \frac{\left[ \left( \frac{\tan \beta \cdot \sigma_{\max}}{\tau_s} \right) - 1 \right]}{\left[ \left( \frac{\sigma_{\max} \cdot a_p \cdot L_t}{F_{nr}} \right) - 1 \right]} \right\} \quad (2)$$

Equation (2) was derived based on the analysis by Boothroyd [4] of the Zorev assumed normal stress distribution model at the tool face in line with equation (2a):

$$\sigma_n = q \cdot x^y \quad (2a)$$

Where  $q$  and  $y$  are constants, and  $x$  is the distance along the tool face from the point where the chip loses contact with the tool [4]. The maximum stress,  $\sigma_{\max}$ , is taken as the ultimate tensile strength of the workpiece material, and  $\tau_s$  is the shear yield strength of the softer material in the chip-tool interaction in the cutting process (i.e., the workpiece material). Equation (2) implies that the sliding-sticking effect at the chip-tool interface in the secondary deformation zone is influenced by the workpiece material properties and tool geometry. Evidence shows that for a selected workpiece material in a cutting operation, the greatest influence is from the tool geometry by way of the rake angle.

The controlled-contact condition of ( $LSL \leq L_t$ ) may appear to deviate from the often assumed condition of ( $LSL = 0.5 \cdot L_t$ ) in the literature - see Hastings, Mathew and Oxley [7] and Stephenson and Agapiou [8]. However, it can be stated that the inequality ( $LSL \leq L_t$ ) can be viewed as implying that the limiting condition for stability is ( $LSL = 0.5 \cdot L_t$ ). Evidently, the limiting controlled-contact state can be arrived at a near optimal ( $LSL \approx 0.5 \cdot L_t$ ) through simulated adjustments to the rake angle only, or the rake angle and feed rate for any workpiece material/tool combination selected for machining. It is posited, in the absence of any support data, that chip formation, behavior, and chip type may be defined by the controlled-contact condition of: ( $LSL \leq L_t$ ).

#### 4.4. Machining Vibration Instability

Approaches to check instability or defining the threshold of chatter due to vibration during the cutting process were conducted through: (i) stability lobe diagram; (ii) critical cutting velocity method advanced by Kovacic [9]; and (iii) chatter tendency factor method suggested by Metcut [10]. A method for analyzing the

possibility of instability due to imbalance, which might result in interrupted cuts, was also considered by Jack [3].

#### 4.5. Variability Analysis through Generated Graphs

Lathe machines are equipped with minimum and maximum rotational speeds of the spindle, tailored to the power requirements. The concept of variability as applied in the ORTHO-OB- CHATTER computer program can be viewed as Computational Learning (CL), and is guided by the possible changes to an initially selected machining-specific program input or cutting conditions, for cutting speed, feed, depth-of-cut, cut or back-engagement, at selected tool geometry conditions of rake angle, and clearance angle. In the program, corresponding *alternate output variables* such as generated forces, temperatures, tool wear, tool-life, economic costs, amongst several others, linked to initial inputs are *automatically generated and translated also to graphical outputs as functions of cutting speed, feed, depth-of-cut or back-engagement, rake angle, chip thickness ratio, and clearance angle*. In the current state of the program, this option is available for the program module of the flow-chart shown in Fig. (1). For graphical outputs, all modules' options can be integrated or consolidated into the format shown in Fig. (1). The generated alternative for other cutting and tool geometry conditions called, TEST POINTS, in the program, are based on the following variables progression analysis of the Cutting speed,  $N$ , that is: Geometric, Arithmetic and Logarithmic progressions multiplier factors equations as given by Sen and Bhattacharyya [11].

#### 4.6. Decision Support Reports Sheets

For each computation worksheet, the ORTHO-OB- CHATTER computer program automatically generates input and output reports. To facilitate decision-making for engineering analysis and recommendations, output reports are available separately for analysis of the following aspects: the mechanics of the metal cutting process, temperatures and thermal effects, vibration and stability, machining economics, wear, and fracture.

### 5. Mechanistic Modeling Through Controlled-Contact

A shortcut to machining workshop, pre- and post-evaluation of a job at hand can be aided by the use of Mechanistic models that define the corresponding cause and effect relationship(s) by which one or more of the cutting conditions (feed rate, cutting velocity, depth of cut or back-engagement, and tool rake angle) are used to predict key parameters such as the likely cutting forces,

temperatures, wear and tool life, within acceptable error or uncertainty limits in engineering practice. The method allows for analysing and finding patterns in data derived from a Statistical Optimization Approach through analysis of probable generated Cutting Forces, Temperatures, Flank Wear and Tool Life through controlled-contact (i.e. ensuring that the relationship  $LSL \leq Lt$  holds) of a population of 270 datasets within recommended cutting velocities and tool rake angles geometry validity ranges, whilst machining various Workpieces using different Cutting Tools as aid for development of a SMART quick-guide machinists assistance Metal Cutting Databank. The selection of data spread for the cutting conditions, in particular the tool rake angle, is linear and/or non-linear, in order to ensure that the controlled-contact stability condition ( $LSL \leq Lt$ ) is fulfilled. A three-point statistical estimation approach is applied, and phenomenally, for every workpiece material/cutting tool combination in the cutting process, there exists a rake angle for which the limiting controlled-contact state ( $LSL \approx 0.5.Lt$ ) can be arrived at near optimally through simulated adjustments to the rake angle only, or rake angle and feed rate. The approach to development of the mechanistic models is related to a defined form factor, ( $ffa = U/\tau$ ), that is the specific cutting energy -to- shear plane yield shear stress ratio; and the functional dependence of the cutting strain on the chip compression ratio, or chip reduction coefficient,  $(1/rc)$ , and rake angle,  $\alpha_n$ , by the Chatterpadhyay [12] given relationship,  $\epsilon_s = [(1/rc) - \tan\alpha_n]$ , which can be expressed as:  $\epsilon_s = (ffa + \tan\alpha_n - 1)$ .

Approaches to estimating specific cutting energy,  $U$ , with support data are available from various sources in the literature. The equation for one approach is shown in the flowchart, and the support data are obtainable from Groover [13], Shaw [1], or the Machining Data Handbook by Metcut [10]. An estimate for the yield shear stress on the shear plane,  $\tau$ , can be made by the suggested approach by Black [14] in the American Society of Metals (ASM) Machining Handbook, based on the method of S. Ramalingam and K. J. Trigger's chart. Jack [3] derived curve-fit model equations applicable for different workpiece material classes based on data extracts from the graphical plots presented in the ASM Machining Handbook, for ease of application in computational studies. Mathematically, mechanistic model equations serve as feedback checks or feedback loadings, where fractions of the input cutting conditions are used to predict specific outputs. That is, mechanistic models show that the generated cutting forces, temperatures in the primary and secondary plastic deformation zones, wear, and tool life depend on the nonlinear interactions of the cutting conditions. Mechanistic models are useful in selecting the right-sized machine tool in terms of power/energy

requirement, cutting tool, cutting velocity, and feed rate for a near-stable metal cutting operation [3]. The descriptions of the considered mechanistic models are presented below.

### 5.1 Cutting Forces

The forms of model nonlinear equations for cutting forces evaluated are:

$$\left. \begin{aligned} F_c &= C_{F_5} \cdot a_p^{w_5} \cdot f^{w_6}; \\ F_t &= C_{F_6} \cdot a_p^{w_7} \cdot f^{w_8}; \end{aligned} \right\} \quad (3)$$

$$\left. \begin{aligned} F_c/a_p &= C_1 \cdot a_c^{a_1} \cdot V^{b_1} \cdot (1 - \sin \alpha_n)^{c_1} \\ F_t/a_p &= C_2 \cdot a_c^{a_2} \cdot V^{b_2} \cdot (1 - \sin \alpha_n)^{c_2} \\ F_{nr}/a_p &= C_3 \cdot a_c^{a_3} \cdot V^{b_3} \cdot (1 - \sin \alpha_n)^{c_3} \\ F_f/a_p &= C_4 \cdot a_c^{a_4} \cdot V^{b_4} \cdot (1 - \sin \alpha_n)^{c_4} \end{aligned} \right\} \quad (4)$$

Stephenson and Agapiou [8] reported the form of equation (4) due to the work of Stephenson and Bandyopadhyay for the estimation of only the normal and friction forces, by which the results obtained can then be applied to the determination of the main tangential and feed forces. Jack [3] extended the method to directly compute the main tangential and feed forces. Evidence shows that equation (4) gives better results with minimal uncertainty in estimating cutting forces, in comparison to using equation (3).

From the evaluation of several workpiece material classes, Jack [3] also showed that the more appropriate models' forms for the determination of cutting forces are:

$$\left. \begin{aligned} F_c/a_p &= C_1 \cdot a_c^{a_1} \cdot (1 - \sin \alpha_n)^{c_1} \\ F_t/a_p &= C_2 \cdot a_c^{a_2} \cdot (1 - \sin \alpha_n)^{c_2} \\ F_{nr}/a_p &= C_3 \cdot a_c^{a_3} \cdot (1 - \sin \alpha_n)^{c_3} \\ F_f/a_p &= C_4 \cdot a_c^{a_4} \cdot (1 - \sin \alpha_n)^{c_4} \end{aligned} \right\} \quad (5)$$

Thus, equation (5) indicates that there is no effect of the cutting velocity on cutting forces.

### 5.2 Temperature Distribution

The forms of model nonlinear equations for temperature distributions evaluated are:

$$\left. \begin{aligned} \theta_s &= C_{F_1} \cdot V^{w_1}; \\ \theta_{\max} &= C_{F_2} \cdot V^{w_2}; \\ \theta_s &= C_{F_3} \cdot f^{w_3}; \\ \theta_{\max} &= C_{F_4} \cdot f^{w_4} \end{aligned} \right\} \quad (6)$$

$$\theta_{\max} = C_{F_7} \cdot V^{w_9} \cdot f^{w_{10}} \quad (6a)$$

### 5.3 Surface Roughness

The form of the model nonlinear equation for the actual surface roughness,  $R_a$ , evaluated is:

$$R_a = C_{F_9} \cdot f^{w_{13}} \cdot V^{w_{14}} \quad (7)$$

The estimation of actual surface roughness,  $R_a$ , is based on the theoretical or ideal surface roughness,  $R_{th}$ , as given by equation (8), and a cutting efficiency factor,  $r_a$ , which is dependent on the workpiece material type and defined as a measure of the closeness of the actual to the ideal surface roughness [13].

$$R_{th} = \frac{0.0321 \cdot f^2}{r_E} \quad (8)$$

Thus,

$$R_a = r_a \cdot R_{th} \quad (9)$$

Groover [13] presented graphical data based on the work of the General Electric (GE) Company to aid estimation of the cutting efficiency factor,  $r_a$ . Extracts from the Groover [13] reported GE graphical data were curve-fitted by Jack [3] for various workpiece materials. One such derived equation applicable to Ductile Metals Modeling (DMM) is given in equation (10):

$$r_a = 2.1798 \cdot e^{-0.02785 \cdot V} + 1.0583 \equiv [2.1798 \cdot \exp(-0.02785 \cdot V)] + 1.0583 \quad (10)$$

The error or uncertainty in prediction is 1.91 percent. Other cutting efficiency factors,  $r_a$ , models applicable to other material classes are available from Jack [3].

### 5.4 Flank Wear

The form of the model nonlinear equation for flank wear,  $VB$ , evaluation is:

$$VB = C_{F_8} \cdot V^{w_{11}} \cdot TL^{w_{12}} \quad (11)$$

A number of tool flank wear models were reported by Jack [3]. One such model based on curve-fit of data obtained from Boothroyd [4] graphical plot of a carbide cutting tool at a reference cutting speed of (1 m/s) is,

$$V_B = 0.0027175 \cdot t_m + 0.02472 \quad (12)$$

Equation (12) can be adjusted to apply to other cutting speeds, and taken as generic (i.e., applicable to other tool types) provides useful results. The Tool-Life (TL) model applied in equation (11) was based on optimum tool life for minimum production time,  $t_p$ , which, according to Boothroyd [4], for practical

application, is a function of the tool changing time,  $t_{ct}$ . The minimum production time is taken as equivalent to machining time,  $t_m$ . The Boothroyd [4] suggested relations are: for High Speed Steel (HSS), ( $t_p = 7 t_{ct}$ ); for carbide tools, ( $t_p = 3 t_{ct}$ ); and for ceramic tools, ( $t_p = t_{ct}$ ). The suggestions of Boothroyd [4] are based on Taylor's tool life constant,  $n = 0.125$  for HSS;  $n = 0.25$  for carbide tools, and  $n = 0.5$  for ceramic tools.

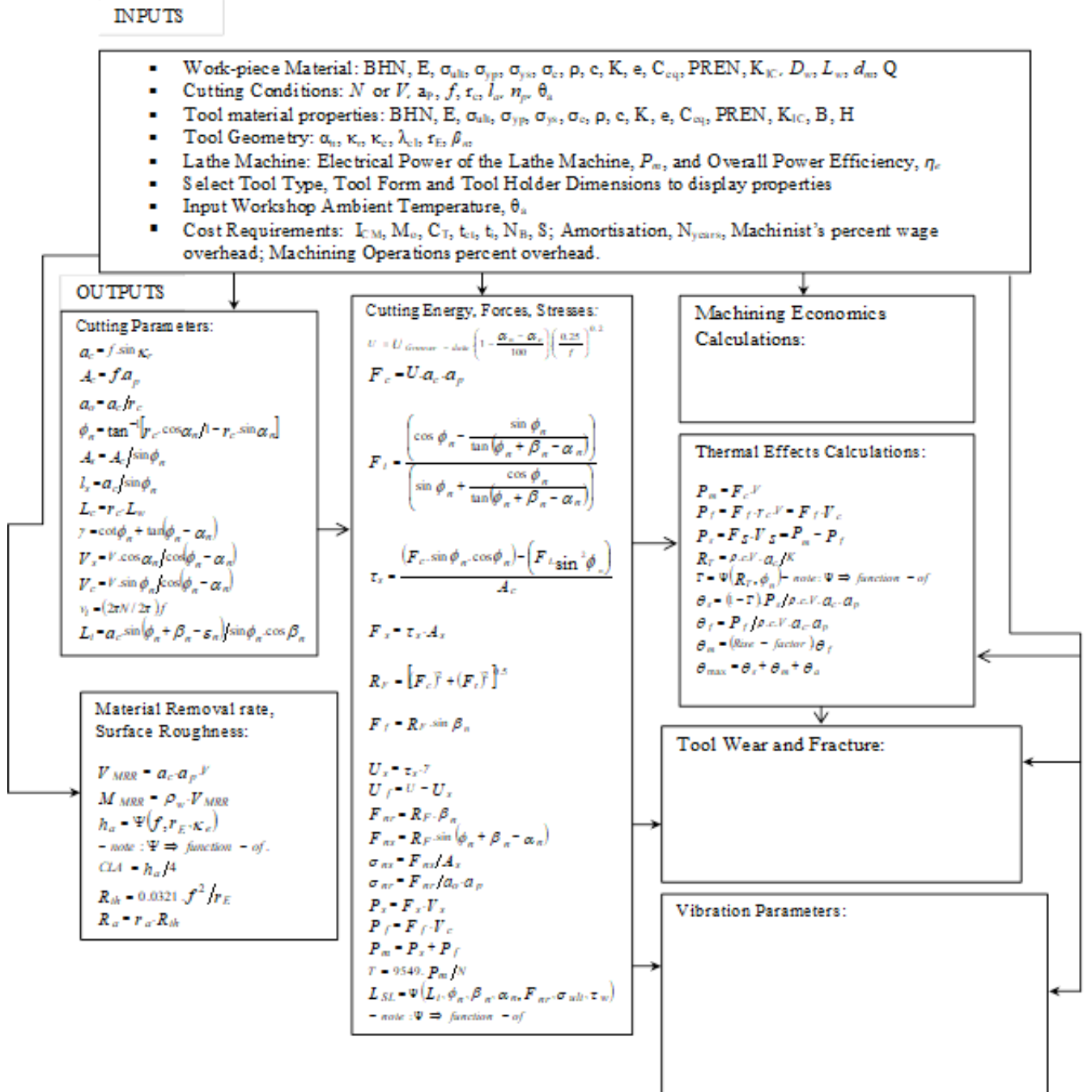


Fig. 1. A Flowchart for Prediction of Metal Cutting Parameters by Turning Operations

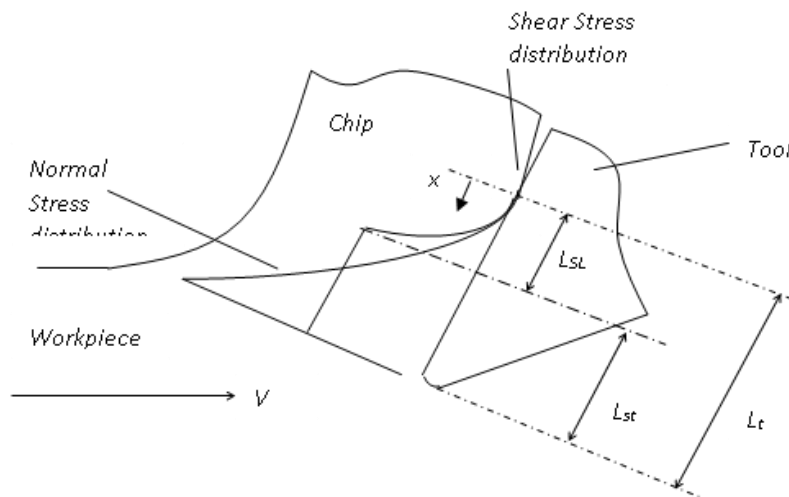


Fig. 2. Model of Chip and Cutting Tool Friction in Orthogonal Cutting (After: [4])

## 6. Validations and Verifications

In Table 1, the ORTHO-OB CHATTER computer program predicted output results validity checks in machining AISI 4130 Alloy steel based on representative cutting data provided by Shaw [1] in estimation of cutting forces in line with the module flow-chart model in Fig. (1). AISI 4130 cold-drawn and Annealed alloy steel workpiece material properties applied for the validation are:

Brinell Hardness Number (BHN) = 201;  
 $\sigma_{ult} = 675.69$  MPa;  $\sigma_{yp} = 599.84$  MPa;  
 $\rho_w = 7800$  kg/m<sup>3</sup>;  $kw = 43$  W/m.DegC;  
 $C_{pw} = cpw = 470$  J/kg.DegC.  
 The cutting conditions as given by Shaw [1] are:  
 $f = 0.064$  mm,  $a_p = 12.1$  mm,  $\alpha_n = 25$  deg.,  
 $V = 27$  m/min. and,  $rc = 0.358$ .

Varied results of uncertainties are achieved with other program modules in machining AISI 4130 alloy steel, some with reduced prediction errors, and others with predictions that are significantly different from the experimental representative data reported by Shaw [1]. Tables 2 and 3 show selected mechanistic model validation checks for main cutting force,  $F_c$ , and feed force,  $F_t$ , respectively, when machining a Cold Drawn AISI 1010 workpiece metal round using a High Speed Steel (HSS) cutting tool when applying equations (3) and (4). Table 4 shows validation and verification checks for tool-face temperature,  $\theta_{max}$ . Table 5 shows the grouped corner or nose radius evaluation statistical method to selecting the best tool type from amongst various corner radiuses within the range: ( $0.4 \text{ mm} \leq r_E \leq 2.4 \text{ mm}$ ), for

cutting conditions of:  $f = 0.3$ mm,  $a_p = 2.5$  mm,  $\alpha_n = 0$  deg. and  $V = 35, 36.5, 38.5, 41.5, 45.5$  and  $50$  m/min.

It is seen that a cutting tool with a corner radius of ( $r_E = 2$  mm) gives the least uncertainty or error, and can be selected for the cutting operation. On the other hand, when statistically evaluated separately with a fixed corner or nose radius across all datasets, as shown in Tables 6 - to- 11, there are no many changes in uncertainty in prediction, but, the choice of selection of nose radius to give the best surface finish hovers between ( $r_E = 2$  mm) and ( $r_E = 2.4$  mm). Indicating that the selection from the group statistical analysis of ( $r_E = 2$  mm) is acceptable. Table 5 also gives details of flank wear data obtainable from a set minimum production time for tool life with a tool changing time of ( $t_{ct} = 2.15$  min.). Expected tool changing times for various types of lathe machine tools were reported by Childs, Maekawa, Obikawa, and Yamane [15].

The Cold Drawn AISI 1010 metal workpiece material properties are:

Brinell Hardness Number (BHN) = 129;  
 $\sigma_{ult} = 537.79$  MPa;  $\sigma_{yp} = 271.93$  MPa;  $\rho_w = 7870$  kg/m<sup>3</sup>;  
 $kw = 49$ W/m.DegC;  $C_{pw} = cpw = 595$  J/kg.DegC. ,  
 $\theta_a = 20$  °C.

The constant coefficients and exponents applicable for machining AISI 1010 material, as derived from mechanistic modeling by Jack [3], are:

$$\left. \begin{aligned} F_c &= 1023.42 \cdot a_p^1 \cdot f^{0.8} \\ F_t &= 393.99 \cdot a_p^1 \cdot f^{0.8} \end{aligned} \right\} \quad (13)$$

The absolute error or uncertainty in the prediction of  $F_c$  and  $F_t$ , by equation (13), are: 2.44 percent and 7.69 percent, respectively.

$$\left. \begin{aligned} F_c/a_p &= 1060.84 \cdot a_c^{0.8} \cdot (1 - \sin \alpha_n)^{0.5583} \\ F_t/a_p &= 441.01 \cdot a_c^{0.8} \cdot (1 - \sin \alpha_n)^{1.7525} \end{aligned} \right\} \quad (14)$$

The absolute error or uncertainty in the prediction of  $F_c$  and  $F_t$ , by equation (14), are: 0.02 percent and 0.007 percent, respectively.

$$\theta_{\max} = 178.19 \cdot V^{0.3043} \cdot f^{0.1915} \quad (15)$$

The absolute error or uncertainty in the prediction of  $\theta_{\max}$  by equation (15) is: 0.304 percent.

$$R_a = (4.087E + 06) \cdot f^2 \cdot V^{-4.9274} \quad (16)$$

The absolute error or uncertainty in group data prediction of  $R_a$ , by equation (16), is 20.06 percent.

$$VB = (1) \cdot V^{0.3748} \cdot TL^{-0.0782} \quad (17)$$

The absolute error or uncertainty in the prediction of  $VB$ , by equation (17), is: “0.00” - percent.

Table 5 indicates that the cutting condition to be selected is guided more by an iterative process, considering the surface roughness and flank wear results, given that Kendall [16] recommended a limit of 1.5 mm for flank wear for High Speed Steel (HSS) tools.

In which case, the matching cutting conditions are:

$$V = 35 \text{ m/min.}, f = 0.3 \text{ mm}, a_p = 2.5 \text{ m}, \alpha_n = 0 \text{ deg.}, \text{ and, } rE = 0.4 \text{ mm.}$$

But, the group statistical evaluation indicates that the best option in terms of surface roughness is one with:

$$V = 45.5 \text{ m/min.}, f = 0.3 \text{ mm}, a_p = 2.5 \text{ m}, \alpha_n = 0 \text{ deg.}, \text{ and, } rE = 2 \text{ mm.}$$

Thus, the decision burden for the manufacturing engineer is determining whether to opt for tool replacement or to prioritize longer tool life for a good surface finish.

**Table 1 - Validation checks for Cutting Forces, when machining AISI 4130 workpiece material round using High Speed Steel (HSS).**

S/N	Cutting Conditions				Cutting Forces, (N)					
	V m/min.	f mm/rev	$a_p$ (mm)	$\alpha_n$ (deg.)	Expt. $F_c$	Pred. $F_c$	Error (percent)	Expt. $F_t$	Pred. $F_t$	Error (percent)
1.	27	0.064	12.1	25	1690	1678.04	0.708	996	992.25	0.377

**Table 2 - Validation checks for Main Cutting Force,  $F_c$ , when machining AISI 1010 workpiece material round using High Speed Steel (HSS).**

S/N	Cutting Conditions				Main Cutting Force, $F_c$ (N)				
	V m/min.	f mm/rev	$a_p$ (mm)	$\alpha_n$ (deg.)	Expt. $F_c$	$F_c$ by eq. (3)	Error (percent)	$F_c$ by eq. (4)	Error (percent)
1.	35	0.3	2.5	0	1012.40	976.54	3.542	1012.25	0.015
2.	36.5	0.35	2.5	0	1145.28	1104.71	3.542	1145.10	0.016
3.	38.5	0.4	2.5	0	1274.39	1229.25	3.542	1274.20	0.015
4.	41.5	0.3	3.75	0	1518.60	1464.81	3.542	1518.38	0.014
5.	45.5	0.35	3.75	0	1717.92	1657.08	3.542	1717.65	0.016
6.	50	0.4	3.75	0	1911.59	1843.88	3.542	1911.30	0.015
7.	35	0.3	2.5	3.5	976.97	976.54	0.044	977.28	0.032
8.	36.5	0.35	2.5	3.5	1105.19	1104.71	0.044	1105.53	0.031
9.	38.5	0.4	2.5	3.5	1229.79	1229.25	0.044	1230.15	0.029
10.	41.5	0.3	3.75	3.5	1465.45	1464.81	0.044	1465.91	0.031
11.	45.5	0.35	3.75	3.5	1657.79	1657.06	0.044	1658.29	0.030
12.	50	0.4	3.75	3.5	1844.69	1843.88	0.044	1845.23	0.029



13.	35	0.3	2.5	7	941.53	976.54	3.718	941.40	0.014
14.	36.5	0.35	2.5	7	1065.11	1104.71	3.718	1064.95	0.015
15.	38.5	0.4	2.5	7	1185.19	1229.25	3.718	1185.03	0.013
16.	41.5	0.3	3.75	7	1412.30	1464.81	3.718	1412.10	0.014
17.	45.5	0.35	3.75	7	1597.66	1657.06	3.718	1597.43	0.014
18.	50	0.4	3.75	7	1777.78	1843.88	3.718	1777.54	0.013

**Table 3 - Validation checks for Feed Force,  $F_t$ , when machining AISI 1010 workpiece material round using High Speed Steel (HSS).**

S/N	Cutting Conditions				Feed Force, $F_t$ (N)				
	$V$ (m/min.)	$f$ (mm/rev)	$a_p$ (mm)	$\alpha_n$ (deg.)	Expt. $F_t$	$F_t$ by eq. (3)	Error (percent)	$F_t$ by eq. (4)	Error (percent)
1.	35	0.3	2.5	0	420.83	375.95	10.664	420.75	0.019
2.	36.5	0.35	2.5	0	476.06	425.29	10.664	476.00	0.013
3.	38.5	0.4	2.5	0	529.73	473.24	10.664	529.75	0.004
4.	41.5	0.3	3.75	0	631.25	563.93	10.664	631.13	0.019
5.	45.5	0.35	3.75	0	714.09	637.94	10.664	714.00	0.013
6.	50	0.4	3.75	0	794.60	709.86	10.664	794.63	0.004
7.	35	0.3	2.5	3.5	376.79	375.95	0.222	376.75	0.011
8.	36.5	0.35	2.5	3.5	426.24	425.29	0.222	426.25	0.002
9.	38.5	0.4	2.5	3.5	474.29	473.24	0.222	474.25	0.008
10.	41.5	0.3	3.75	3.5	565.18	563.93	0.222	565.13	0.009
11.	45.5	0.35	3.75	3.5	639.36	637.94	0.222	639.38	0.003
12.	50	0.4	3.75	3.5	711.44	709.86	0.222	711.38	0.008
13.	35	0.3	2.5	7	335.11	375.95	12.187	335.00	0.033
14.	36.5	0.35	2.5	7	379.10	425.29	12.184	379.00	0.026
15.	38.5	0.4	2.5	7	421.84	473.24	12.185	421.75	0.021
16.	41.5	0.3	3.75	7	502.67	563.93	12.187	502.50	0.034
17.	45.5	0.35	3.75	7	568.64	637.94	12.187	568.50	0.025
18.	50	0.4	3.75	7	632.75	709.86	12.186	632.63	0.019

**Table 4 - Validation checks for Tool-Face Temperature,  $\theta_{max}$ , when machining AISI 1010 workpiece material round using High Speed Steel (HSS).**

S/N	Cutting Conditions				Tool Temperature, $\theta_{max}$ (°C)		
	$V$ (m/min.)	$f$ (mm/rev)	$a_p$ (mm)	$\alpha_n$ (deg.)	Expt. $\theta_{max}$	$\theta_{max}$ by eq. (6a)	Error (percent)
1.	35	0.3	2.5	0	419.70	417.40	0.548
2.	36.5	0.35	2.5	0	435.17	435.43	0.060
3.	38.5	0.4	2.5	0	451.77	454.02	0.498
4.	41.5	0.3	3.75	0	439.98	439.60	0.086
5.	45.5	0.35	3.75	0	462.96	465.63	0.577

6.	50	0.4	3.75	0	487.65	491.60	0.810
7.	35	0.3	2.5	3.5	419.67	417.40	0.541
8.	36.5	0.35	2.5	3.5	435.98	435.43	0.126
9.	38.5	0.4	2.5	3.5	453.67	454.02	0.077
10.	41.5	0.3	3.75	3.5	440.67	439.60	0.243
11.	45.5	0.35	3.75	3.5	465.08	465.63	0.118
12.	50	0.4	3.75	3.5	491.45	491.60	0.031
13.	35	0.3	2.5	7	418.29	417.40	0.213
14.	36.5	0.35	2.5	7	435.32	435.43	0.025
15.	38.5	0.4	2.5	7	453.97	454.02	0.011
16.	41.5	0.3	3.75	7	439.92	439.60	0.073
17.	45.5	0.35	3.75	7	465.57	465.63	0.013
18.	50	0.4	3.75	7	493.38	491.60	0.361

**Table 5 - Validation checks for Surface Roughness,  $R_a$ , and Flank Wear,  $V_B$  when machining cold-drawn AISI 1010 workpiece material round using High Speed Steel (HSS) at Different Nose radii, and Cutting Speeds.**

S/N	Cutting Conditions					Surface Roughness and Flank Wear					
	$V$ (m/min.)	$f$ (mm/rev)	$a_p$ (mm)	$\alpha_n$ (deg.)	$r_E$ (mm)	Expt. $R_a$ (mm)	$R_a$ (mm) by eq. (7)	Error (percent)	Expt. $V_B$ (mm)	$V_B$ (mm) by eq. (11)	Error (percent)
1.	35	0.3	2.5	0	0.4	0.0136	0.0091	33.088	1.446	1.446	0.000
2.	36.5	0.3	2.5	0	0.8	0.0067	0.0074	10.448	1.508	1.508	0.000
3.	38.5	0.3	2.5	0	1.2	0.0043	0.0057	32.558	1.590	1.590	0.000
4.	41.5	0.3	2.5	0	1.6	0.0032	0.0039	21.875	1.714	1.714	0.000
5.	45.5	0.3	2.5	0	2.0	0.0024	0.0025	4.167	1.880	1.880	0.000
6.	50	0.3	2.5	0	2.4	0.0019	0.0016	15.789	2.066	2.066	0.000

**Table 6 - Validation checks for Surface Roughness,  $R_a$ , when machining Cold drawn AISI 1010 workpiece material round using High Speed Steel (HSS), with Different Cutting Speeds but same Nose Radius,  $r_E = 0.4$  mm.**

S/N	Cutting Conditions					Surface Roughness, $R_a$ (mm)		
	$V$ (m/min.)	$f$ (mm/rev)	$a_p$ (mm)	$\alpha_n$ (deg.)	$r_E$ (mm)	Expt. $R_a$ (mm)	$R_a$ (mm) by eq. (7)	Error (percent)
1.	35	0.3	2.5	0	0.4	0.013584	0.013599	0.110
2.	36.5	0.3	2.5	0	0.4	0.013341	0.013343	0.015
3.	38.5	0.3	2.5	0	0.4	0.013033	0.013024	0.069
4.	41.5	0.3	2.5	0	0.4	0.012601	0.012588	0.103
5.	45.5	0.3	2.5	0	0.4	0.012078	0.012073	0.041
6.	50	0.3	2.5	0	0.4	0.011556	0.011568	0.104

**Table 7 - Validation checks for Surface Roughness,  $R_a$ , when machining Cold Drawn AISI 1010 workpiece material round using High Speed Steel (HSS), with Different Cutting Speeds but the same Nose Radius,  $r_E = 0.8$  mm.**

S/N	Cutting Conditions					Surface Roughness (mm)		
	$V$ (m/min.)	$f$ (mm/rev)	$a_p$ (mm)	$\alpha_n$ (deg.)	$r_E$ (mm)	Expt. $R_a$ (mm)	$R_a$ (mm) by eq. (7)	Error (percent)
1.	35	0.3	2.5	0	0.8	0.0067922	0.0067996	0.109
2.	36.5	0.3	2.5	0	0.8	0.0066707	0.0066714	0.010
3.	38.5	0.3	2.5	0	0.8	0.0065164	0.0065119	0.069
4.	41.5	0.3	2.5	0	0.8	0.0063004	0.0062939	0.103
5.	45.5	0.3	2.5	0	0.8	0.0060392	0.0060366	0.043
6.	50	0.3	2.5	0	0.8	0.0057781	0.0057838	0.099

**Table 8 - Validation checks for Surface Roughness,  $R_a$ , when machining Cold Drawn AISI 1010 workpiece material round using High Speed Steel (HSS), with Different Cutting Speeds but the same Nose Radius,  $r_E = 1.2$  mm.**

S/N	Cutting Conditions					Surface Roughness, $R_a$ (mm)		
	$V$ (m/min.)	$f$ (mm/rev)	$a_p$ (mm)	$\alpha_n$ (deg.)	$r_E$ (mm)	Expt. $R_a$ (mm)	$R_a$ (mm) by eq. (7)	Error (percent)
1.	35	0.3	2.5	0	1.2	0.0045282	0.0045331	0.108
2.	36.5	0.3	2.5	0	1.2	0.0044471	0.0044476	0.011
3.	38.5	0.3	2.5	0	1.2	0.0043443	0.0043412	0.071
4.	41.5	0.3	2.5	0	1.2	0.0042003	0.0041959	0.105
5.	45.5	0.3	2.5	0	1.2	0.0040261	0.0040244	0.042
6.	50	0.3	2.5	0	1.2	0.0038520	0.0038558	0.099

**Table 9 - Validation checks for Surface Roughness,  $R_a$ , when machining Cold Drawn AISI 1010 workpiece material round using High Speed Steel (HSS), with Different Cutting Speeds but the same Nose Radius,  $r_E = 1.6$  mm.**

S/N	Cutting Conditions					Surface Roughness, $R_a$ (mm)		
	$V$ (m/min.)	$f$ (mm/rev)	$a_p$ (mm)	$\alpha_n$ (deg.)	$r_E$ (mm)	Expt. $R_a$ (mm)	$R_a$ (mm) by eq. (7)	Error (percent)
1.	35	0.3	2.5	0	1.6	0.0033961	0.0033998	0.109
2.	36.5	0.3	2.5	0	1.6	0.0033354	0.0033357	0.009
3.	38.5	0.3	2.5	0	1.6	0.0032582	0.0032559	0.071
4.	41.5	0.3	2.5	0	1.6	0.0031502	0.0031470	0.102
5.	45.5	0.3	2.5	0	1.6	0.0030196	0.0030183	0.043
6.	50	0.3	2.5	0	1.6	0.0028890	0.0028919	0.100

**Table 10 - Validation checks for Surface Roughness,  $R_a$ , when machining Cold Drawn AISI 1010 workpiece material round using High Speed Steel (HSS), with Different Cutting Speeds but the same Nose Radius,  $r_E = 2.0$  mm.**

S/N	Cutting Conditions					Surface Roughness, $R_a$ (mm)		
	$V$ (m/min.)	$f$ (mm/rev)	$a_p$ (mm)	$\alpha_n$ (deg.)	$r_E$ (mm)	Expt. $R_a$ (mm)	$R_a$ (mm) by eq. (7)	Error (percent)
1.	35	0.3	2.5	0	2.0	0.0027169	0.0027198	0.107
2.	36.5	0.3	2.5	0	2.0	0.0026683	0.0026685	0.007
3.	38.5	0.3	2.5	0	2.0	0.0026066	0.0026047	0.073

4.	41.5	0.3	2.5	0	2.0	0.0025202	0.0025176	0.103
5.	45.5	0.3	2.5	0	2.0	0.0024157	0.0024146	0.046
6.	50	0.3	2.5	0	2.0	0.0023112	0.0023135	0.100

**Table 11 - Validation checks for Surface Roughness,  $R_a$ , when machining Cold Drawn AISI 1010 workpiece material round using High Speed Steel (HSS), with Different Cutting Speeds but the same Nose Radius,  $r_E = 2.4$  mm.**

S/N	Cutting Conditions					Surface Roughness, $R_a$ (mm)		
	$V$ (m/min.)	$f$ (mm/rev)	$a_p$ (mm)	$\alpha_n$ (deg.)	$r_E$ (mm)	Expt. $R_a$ (mm)	$R_a$ (mm) by eq. (7)	Error (percent)
1.	35	0.3	2.5	0	2.4	0.0022641	0.0022665	0.106
2.	36.5	0.3	2.5	0	2.4	0.0022236	0.0022238	0.009
3.	38.5	0.3	2.5	0	2.4	0.0021721	0.0021706	0.069
4.	41.5	0.3	2.5	0	2.4	0.0021001	0.0020980	0.100
5.	45.5	0.3	2.5	0	2.4	0.0020131	0.0020122	0.045
6.	50	0.3	2.5	0	2.4	0.0019260	0.0019279	0.099

**Table 12 - Validation Checks in Four Modules of the ORTHO-OB CHATTER Computer Program Indicating Consistency of Form Factor Using Data Reported by Marusich [17] in Metal Cutting of Aluminum Alloy AL 6061-T6-T, for:  $f = 0.25$  mm;  $V = 600$  m/min,  $\alpha_n=10$  (deg.).**

Parameter	Experimental Data Taken from Marusich [17] Paper	Method 1	Method 2	Method 3	Method 4
$F_c$ (N)	900	900.11	900.44	901.70	900.46
$F_t$ (N)	270	292.22	292.32	292.73	292.33
$\theta_{max}$ (Deg.C)	400	249.67	432.25	390.83	432.18
$\theta_s$ (Deg.C)	175	93.12	209.14	208.25	173.70
<b>Predicted <math>a_p</math>, (mm)</b>		11.43	4.06	5.12	6.13
$\Phi_n$ , (deg.)	27	27.01	27.01	27.01	27.01
$\beta_n$ , (deg.)		27.99	27.99	27.99	27.99
$U$ (GJ/m <sup>3</sup> )		0.315	0.887	0.704	0.588
$\tau_s$ (MPa)		106.37	300.76	238.83	198.41
<b>Form factor (<math>U/\tau_s</math>)</b>		2.96	2.95	2.95	2.96
<b>Predicted <math>r_c</math></b>		0.475	0.475	0.475	0.475

**Note:** The experimental data in Table 12 were taken from Marusich [17] 's reported graphs; therefore, a reading error may apply.

## 7. Concluding Remarks

Evidence from the myriad of approaches to examining the mechanics of the metal cutting process shows that predictions of metal cutting performance are method and material-specific, and influenced by the approaches adopted to estimating the cutting energy, shear plane angle, and, by implication, the friction angle, and the

shear plane yield shear stress. Interestingly, a phenomenon not yet fully understood from verification tests conducted to predict cutting forces and temperatures for a particular cutting operation of an Aluminium Alloy – AL-6061-T6-T, under a defined set of cutting conditions using data reported by Marusich [17], across the different modules of the ORTHO-OB- CHATTER program shows that regardless of the methods adopted for estimating the

specific cutting energy and the yield shear stress, the form factor, ( $f_{fa} = U/\tau$ ), is constant. See results for the four methods in Table 12. While it has been stated that workpiece material nonlinearity may play a critical role in prediction uncertainties, accurate predictions in line with experimental results within limits for engineering acceptance have been obtained for various workpiece material classes across the ORTHO-OB-CHATTER program modules. Detailed Validation and Verification checks were conducted from selections across all workpiece materials classes using various tool types under varied cutting conditions, and are available in Jack [3]. Validation and Verification checks also indicate that the worksheet program modules' data specificity implies the existence of a suitable module for any cutting operation, as determined through simulated analysis of the desired cutting conditions. Such simulations can be discerned from the variations in the predicted depth of cut/back-engagement shown in the results of Table 12.

It is hoped that for practical industry application in the near future, development of a detailed metal cutting databank through mechanistic reasoning can create awareness to aid developing a sector specific pre-machining plan interactive language processing machinist assistant App by a conversational dialogue system that provides answers to specific questions from the manufacturing engineer and machinist to accelerate product development, reducing workshop trials, and accurately matching parts to be produced with the desirable workpiece material, for sustainable optimal parts production, thereby saving time, energy and costs and hence, improving productivity.

## 8. Conflicts of Interest

There are no conflicts of interest in this publication.

## References

1. M. C. Shaw, *Metal Cutting Principles*, 2nd ed., New York: Oxford University Press, 2005.
2. C. A. van Luttervelt, T. H. C. Childs, I. S. Jawahir, F. Klocke, and P. K. Venuvinod, "Present situation and future trends in modelling of machining operations—Progress report of the CIRP Working Group Modelling of Machining Operations," *Annals of the CIRP*, vol. 47, no. 2, 1998.
3. T. K. Jack, "Nonlinearities in machining: Evaluation of machining parameters and stability predictions in turning operations," Ph.D. dissertation, Dept. Mech. & Aerospace Eng., Univ. of Uyo, Uyo, Nigeria, 2023.
4. G. Boothroyd, *Fundamentals of Metal Machining and Machine Tools*, Auckland: McGraw-Hill, 1975.
5. Chartered Management Institute, *Setting SMART Objectives Checklist*, 2014. [Online]. Available: <https://www.managers.org.uk>
6. R. A. Cookson, *Lecture Notes on Fatigue and Fracture*, School of Mechanical Engineering, Cranfield Institute of Technology (now Cranfield University), SME/PPA/RAC/2188, 1992/1993.
7. W. F. Hastings, P. Mathew, and P. L. B. Oxley, "A machining theory for predicting chip geometry, cutting forces, etc. from work material properties and cutting conditions," *Proc. Roy. Soc. London A*, vol. 371, pp. 569–587, 1980.
8. D. A. Stephenson and J. S. Agapiou, *Metal Cutting Theory and Practice*, New York: CRC Press, Marcel & Dekker Inc., 1997.
9. Kovacic, "The chatter vibrations in metal cutting – theoretical approach," *Facta Universitatis, Mechanical Engineering Series*, vol. 1, no. 5, pp. 581–593, 1998.
10. Metcut Research Associates Inc. Technical Staff, *Machining Data Handbook*, vol. 2, 3rd ed., United States Department of Defence (DOD), Army Materials and Mechanics Research Centre, 1980.
11. G. C. Sen and A. Bhattacharyya, *Principles of Machine Tools*, New Delhi: New Central Book Agency, 2011.
12. B. Chattopadhyay, *Lecture Notes on Analytical and Experimental Determination of Cutting Forces – Lesson 9, Manufacturing Processes II*, Indian Institute of Technology, Kharagpur.
13. M. P. Groover, *Fundamentals of Modern Manufacturing: Materials, Processes and Systems*, 4th ed., New Jersey: John Wiley & Sons, 2010.
14. J. T. Black, "Mechanics of chip formation," in *Handbook of ASM: Machining*, vol. 16, pp. 7–12, 1997.
15. T. Childs, K. Maekawa, Y. Obikawa, and Y. Yamane, *Metal Machining: Theory and Applications*, London: Arnold, 2000.
16. L. A. Kendall, "Tool wear and tool life," in *Handbook of ASM: Machining*, vol. 16, p. 43, 1997.
17. T. D. Marusich, *Proceedings of ASME Congress*, Nov. 11–16, New York (NY), 2001.